

# Vibration-to-Electrical Power Conversion Using High-Aspect-Ratio MEMS Resonators

Johnny M. H. Lee<sup>1</sup>, Steve C. L. Yuen<sup>2</sup>, Mimi H. M. Luk<sup>3</sup>, Gordon M. H. Chan<sup>1</sup>, King Fong Lei<sup>1</sup>,  
Wen J. Li<sup>1,\*</sup>, Philip H. W. Leong<sup>2</sup>, and Yeung Yam<sup>3</sup>

<sup>1</sup>Centre for Micro and Nano Systems, The Chinese University of Hong Kong, Hong Kong SAR  
<sup>2</sup>Dept. of Computer Science and Engineering, The Chinese University of Hong Kong, Hong Kong SAR  
<sup>3</sup>Intelligent Control Systems Laboratory, The Chinese University of Hong Kong, Hong Kong, SAR

## ABSTRACT

This paper presents the design and experimental results of a Micro Power Generator (MPG) which harvests mechanical energy from its environment and converts this energy into useful electrical power. The energy transduction component is mainly a magnet and a resonating spring made using SU-8 molding and MEMS electroplating technologies. We have shown that when the MPG is packaged into an AA battery size container along with a power-management circuit that consists of rectifiers and a capacitor, it is capable of producing ~1.6V DC when charged for less than 1min. Our goal is to realize a MPG to function with low input mechanical frequencies while produce enough power for low-power wireless applications.

**Keywords:** micro power generator, micro energy transducer, high-aspect-ratio MEMS, SU-8 processing.

## INTRODUCTION

Shelf life, replacement accessibility, and potential hazards of chemicals are some of the problems when chemical batteries are used. Our ongoing work is to develop a new power supply that has extreme-long shelf life, is environmentally safe, and can harvest and convert environmental energy into electrical power. Essentially, we want to produce a micro power transducer capable of converting mechanical energy from a working environment into useful electrical energy for applications in wireless sensing and signal transmission. Three main advancements in engineering technology in the last 15 years will allow possible applications for magnetic-induction based *micro* energy transducers in the future: 1) increase in magnetic flux density of production grade rare-earth-magnets; 2) continual reduction in power consumption of circuit and sensors; 3) development of MEMS fabrication technologies that will allow precise and low cost production of micro spring-mass systems.

Micro power generators operating using various physical principles have been studied recently (for a comprehensive survey, see [1]). As far as mechanical energy harvesting, Williams and Yates have developed an MEMS-based electromagnetic generator to produce 0.3 $\mu$ W in 1997 [1], and Amirtharajah and Chandrakasan

used a *macro* vibration-based power generator to drive a signal processing circuitry in 1998 [3]. Nevertheless, neither of the groups was able to demonstrate a micro power generator capable of producing enough power to drive an off-the-shelf wireless circuit. Our group later demonstrated a 1cm<sup>3</sup> vibration-based energy converter capable of powering an off-the-self IR transmitter [4] (2000) and RF transmitter [5] (2002). In that work, the energy converting transducer was made of copper (Cu) springs fabricated using a Nd:YAG laser micromachining system, which limited the reduction and precision of the spring dimensions. In this paper, we will present our recent results in creating an energy transducer using MEMS compatible SU-8 fabricated high-aspect-ratio Cu springs to amplify input mechanical vibrations from the transducer's environment.

## SU8 BASED MEMS RESONATOR

### Fabrication Process

The dimensions for the Cu resonator were determined using a dynamic simulation as described in the next section. Then, an SU-8 based electroplating technique (Figure 1) was used to fabricate the springs as presented below. The fabrication process starts with a polymethylmethacrylate (PMMA) substrate. The Cr/Au (500Å/2000Å) seed layers are deposited on a PMMA substrate by E-beam deposition. SU-8, a negative thick photoresist (PR), is deposited on the PMMA by spin-coating (100-150 $\mu$ m thick). The resist is soft baked in an oven at 40°C for 2 days. After that, the resist is exposed with 400nm UV under a mask with the designed spring patterns for 20 minutes. Following the exposure, the resist is developed in SU-8 developer for 10-15 minutes at room temperature with mild agitation and rinsed with isopropyl alcohol. The above processes create the thick SU-8 mold on a PMMA substrate as shown in Figure 1d. Then, the mold is used to electroplate Cu with a current density of 40mA/cm<sup>2</sup> for 1.5 hours. A 100 $\mu$ m thick Cu spring resonator can be fabricated in the SU-8 mold using the above parameters. Finally, the SU-8 resist and PMMA substrate are separated using the MicroChem Remover, resulting in isolated Cu spring resonators as shown in Figure 2.

## RESONATOR CHARACTERISTICS

The motion of the spring-mass under a mechanical input vibration is similar to those reported in our prior work for laser-micromachined springs [5], i.e., 3 distinctive modes of resonance were observed. These 3 different modes of resonant vibration were captured using a digital video camera and analyzed. A strobe light

\*Contacting Author: wen@acae.cuhk.edu.hk; CMNS, The Chinese University of Hong Kong; MMW Bldg., Room 422; Shatin, NT; Hong Kong SAR. This project is funded by a grant from the Hong Kong Innovation and Technology Commission (ITF/185/01).

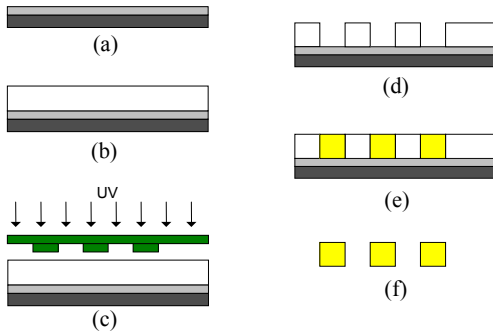


**Figure 1.** SU-8 based Cu resonator fabrication process. (a) Sputter Cr/Au seed layers on PMMA substrate; (b) coat thick SU-8 negative PR and soft bake; (c) expose SU-8 PR with spring pattern mask using UV light source; (d) develop in SU-8 developer; (e) electroplate copper into the SU-8 mold; (f) strip SU-8 and PMMA substrate by MicroChem Remover.

was used to synchronize the vibration motion of the mass. Sample frames from the digital movies are shown in Figure 3 which shows the 3 modes of vibration. The 1<sup>st</sup> mode is a vertical resonance. For the 2<sup>nd</sup> and 3<sup>rd</sup> modes, the mass appeared to cyclically rotate about an axis parallel to the plane of the coil. Most interestingly, the voltage output at the 2<sup>nd</sup> and 3<sup>rd</sup> modes of resonance for the generator is higher than the 1<sup>st</sup> mode resonance. Physically, this can be explained by the fact that Faraday's Law predicts the voltage output to be proportional to the rate of changing magnetic flux, and hence, faster the movement of the mass, the greater the current induction. It was observed that the vibration amplitude of the rotation was very small compared to the vertical vibration at the 1<sup>st</sup> mode resonance. Hence, if the a spring can be designed to vibrate in a horizontal plane with rotation, rather than to vibrate in a vertical direction relative to a coil, the voltage output can be increased and the stress on the spring can be reduced.

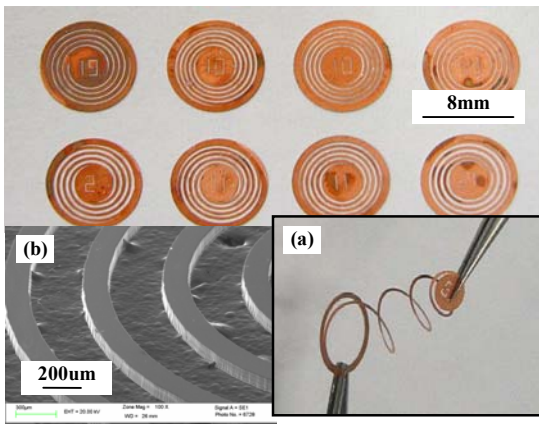


**Figure 2.** Batch fabricated Cu resonators. Inset (a) shows a spring being stretched. Inset (b) shows an SEM picture of a SU8-fabricated resonator.

## SIMULATION AND MODELING

### FEA Modeling of the MEMS Resonators

Finite element analysis was used to study the vibration characteristics of different geometric configurations and spring designs. The copper

resonating spring and magnet were modeled using ALGOR as shown in Figure 3a. With the use of linear modal analyses, the vibration resonances of the micro spring-mass were extracted from the simulation. Vertical translation vibration was observed in the first mode as indicated in Figure 3b. In the second and third modes, horizontal rotational movements were observed (Figure 3c and 3d). The geometric values and material properties used in the analyses are provided in Table 1 and an average of 15% deviation was identified between the simulated resonant frequencies and experimental measurements. As indicated in Table 1, a decline of resonant frequencies is observed with narrowing spring gap, which can be explained by the decrease of spring constant resulted from the increased total spring length. Besides, by comparing the resonant frequencies resulted from a bi-spiral (two spiral springs) and single spiral (see Figure 4) springs in identical configurations, a significant reduction of vibration frequencies is observed, which can be explained by the considerable decrease of spring constant caused by the increase of spring length and reduction of spring cross-section area.

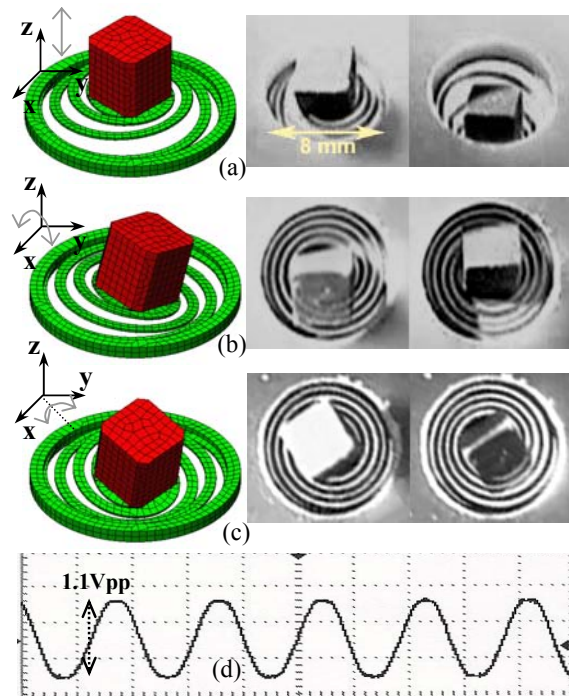


**Figure 3.** Simulation and experimental results for 3 different resonance vibration modes are matched: (a) 1st mode vibration (vertical); (b) 2nd mode vibration (horizontally along x axis); (c) 3rd mode vibration (horizontally along an axis between x and y axis); (d) Output waveform of the micro power transducer produces a voltage output of 1.1Vpp at 111 Hz (3<sup>rd</sup> mode). The capacitor charged up to 1.65V DC in about one minute. The MPG was connected with the power management circuit and a 100k ohm resistance.

### MPG System Modeling

To model different behaviors of the MPG due to electro-mechanical coupling effects, basic principles of electromagnetic theory are adopted. According to the Faraday's Law of induction, a voltage is induced in a coil when there is a change of magnetic flux through the

loop of coil. This induction behavior is contributed by the mass-spring resonator structure in the micro transducer, where a magnet is attached to a spring and moves through a coil which is fixed on the housing of the device. This is depicted in Figure 5.

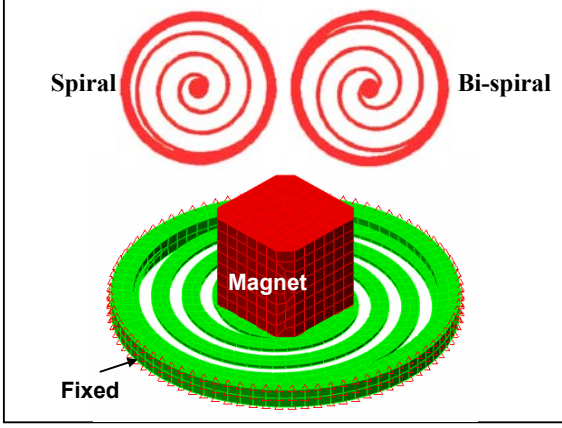


Figure 4. Finite element model of the micro resonating spring.

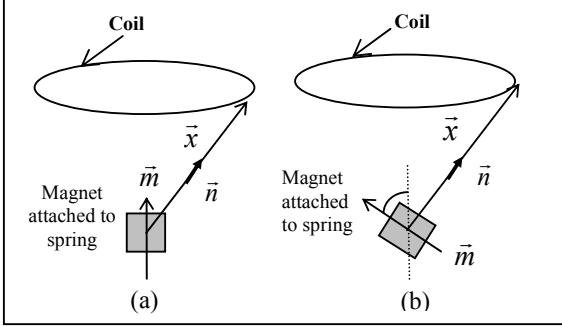


Figure 5. Motion of the mass-spring resonator structure through the coil : (a) Translational motion; (b) Rotational motion.

The induced emf in the coil is given by Faraday's Law as:

$$V = -N \frac{d\phi}{dt} \quad (1)$$

where  $N$  is the number of turns of coil and  $\phi$  is the flux. The flux  $\phi$  is defined by:

$$\phi = \vec{B}(\vec{x}) \cdot \vec{A} \quad (2)$$

where  $\vec{A}$  is the vector area of the loop of coil, and  $\vec{B}(\vec{x})$  is the magnetic field at the coil at a distance  $x$  from the magnetic dipole, which is given by:

$$\vec{B}(\vec{x}) = \frac{\mu_0}{4\pi} \frac{(3\vec{n}(\vec{n} \cdot \vec{m}) - \vec{m})}{|\vec{x}|^3} \quad (3)$$

Here,  $\vec{m}$  represents the magnetic dipole moment of the magnet,  $\vec{n}$  is the unit vector in the  $\vec{x}$ -direction, and  $\mu_0$  is the permeability constant. Based on the above expressions, an electro-mechanical model was implemented in MATLAB such that different magnitudes of induced emf could be obtained by varying the orientations and movements of the magnetic dipole moment. Results of different configurations can also be analyzed. Thus, the model serves as the basis for system level optimization. As an example, an SU-8 fabricated spring with parameters given in Figure 6 was experimentally tested and compared with the modeled results using the model. As indicated in Figure 6, the experimental and modeled results matched well in terms of output voltage amplitude. However, the predicted output frequency has slight variation from the experimental results (i.e., 167.8Hz for experimental and 176Hz from modeling). We conjecture that this is mainly due to the location of the magnet on the Cu resonator, which is not well-controlled in our current packaging process.

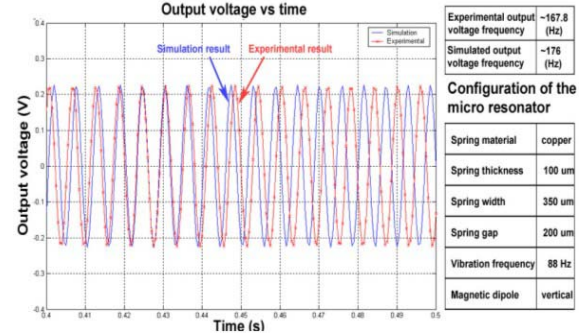


Figure 6. Comparison of experimental and modeled results at 1<sup>st</sup> mode resonance. Note that the transducer mechanical resonance is ~88Hz, but the voltage output is 2 times this frequency due to the up and down motion of the mass-spring through the coil.

Table 1. Finite element simulated resonance of different spring geometric configurations.

| Spring type         | Spring diameter (mm) | Center platform diameter (mm) | Spring width ( $\mu\text{m}$ ) | Spring gap ( $\mu\text{m}$ ) | Simulated resonant modes and frequencies (Hz) |            |            |     |
|---------------------|----------------------|-------------------------------|--------------------------------|------------------------------|---|------------|------------|-----|
|                     |                      |                               |                                |                              | *Experimentally measured values               |            |            |     |
|                     |                      |                               |                                |                              | 1   | 2          | 3          | 4   |
| Bi-spiral           | 7                    | 3.5355                        | 350                            | 350                          | 102 (86*)                                     | 126 (102*) | 128 (111*) | 598 |
|                     |                      |                               |                                | 200                          | 88 (76*)                                      | 107 (98*)  | 112 (104*) | 527 |
| Bi-spiral<br>Spiral | 7                    | 1                             | 200                            | 800                          | 68  | 124        | 143        | 388 |
|                     |                      |                               |                                |                              | 37  | 75         | 80         | 218 |
| Bi-spiral<br>Spiral | 5                    | 3                             | 200                            | 400                          | 174   | 183        | 209        | 639 |
|                     |                      |                               |                                |                              | 65  | 74         | 80         | 225 |

Spring thickness = 100 $\mu\text{m}$ ; Magnet weight = 200mg; Material properties of spring (copper): Mass density = 8902.3kg/m<sup>3</sup>; Modulus of elasticity = 117.21GPa; Poisson's ratio = 0.330; Shear modulus of elasticity = 44.126GPa; Material properties of magnet: Modulus of elasticity = 158.58GPa; Poisson's ratio = 0.275; Shear modulus of elasticity = 62.190GPa;

## AA SIZE BATTERY PACKAGING

We are now developing a MPG integrated with a power-management circuit with total dimension equal to an AA-size battery. The dimensions and composition of the components inside the AA-size “power-conversion cell” is given in Figure 6. Some experimental results have been obtained for this power-conversion cell and are presented below.

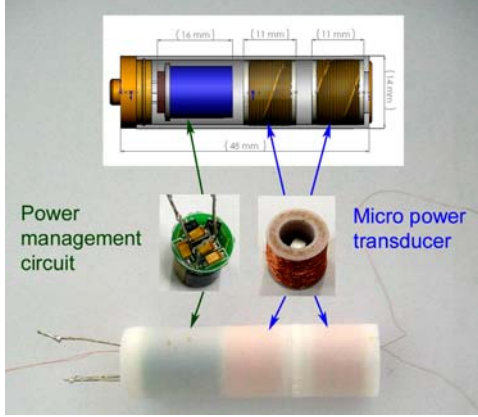


**Figure 7.** The AA-size micro power generator which consists of two transducers and a power management circuit.

### Experimental Results

To test the power-conversion cell, a 100kΩ resistor was connected to the capacitor of the power management circuit, and the potential difference across the resistor was measured. The capacitor was charged to about 1.55V at 1st mode and 1.65V at 3rd mode (within ~1min). Using these values, we calculated the power output for the transducer when loaded with a 100kΩ resistor is ~24μW at 1st mode and ~27μW at 3rd mode, respectively. Without the power management circuit, the micro power transducer produced a voltage output of 1.34Vpp AC at 85 Hz (1<sup>st</sup> mode), and a voltage output of 1.44Vpp AC at 111 Hz (3<sup>rd</sup> mode). The results given above were obtained using only 1 transducer for the cell. A maximum of 2 transducers can be packaged in a power-conversion cell with our current design.

## APPLICATIONS

### RF Wireless Circuits for ID Tagging

We have already shown that a 1cm<sup>3</sup> MPG is capable of driving IR [4] and RF [5] wireless transmission circuit. Currently, we are developing a circuit system for RF wireless transmission applicable for ID tagging using the AA-size MPG. This new circuit system consists of 1) a voltage rectifier, charge pump regulator and 3V comparator, 2) uP, 3) NVRAM, RTC, Temperature and iMems accelerometer, and 4) RF Transmitter. A voltage tripler is used to step up the input voltage to >0.9V DC. This is a passive circuit which can operate at voltages lower than a normal MOS transistor’s threshold voltage. A charge pump

regulator further steps up the output of multiplier to 3.3V and charges up the reservoir capacitor Cres. To save power, the microprocessor controls the power supplies for peripheral chips and only applies power via an analog switch when required. The microprocessor is in sleep mode until the voltage level of Cres rises to 3.3V when it will be awaked by the 3V comparator.

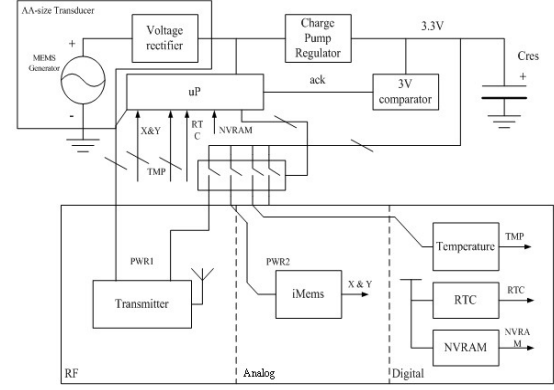


**Figure 8.** Circuit schematic for the proposed RF ID tagging wireless transmission system.

### Centrifugally Generated Power Applications

We have also modified the MPG to generate power in rotating conditions. Potential applications for this MPG configuration include any electronic devices implanted in mechanical systems that undergo rotation, e.g., automobile tires, rotary machinery... etc. With a suitable orientation, we have shown that a 1cm<sup>3</sup> transducer is able to produce 2.5Vpp when it is housed on an 8cm diameter disc rotating at 4500rpm. With appropriate power management circuit, this voltage output is sufficient to drive the low-power IC circuit systems we demonstrated in [5]. Basically, besides picking up vibrations from rotating machineries, the MPG can also be used to convert the mechanical motion of the spring-magnet caused by the imbalance of centrifugal and gravitational forces acting on it into electrical energy, as the MPG undergoes rotation.

#### Force Balance on a Rotating MPG

Referring to Figure 9, the gravitation force acting along a spinning disk reference line is:

$$F = mg \cos \gamma \sin \omega t \quad (1)$$

For the MPG illustrated in the figure, the motion of the magnet along the disk reference line due to gravity can be described by:

$$m\ddot{x} + \frac{\beta k}{\omega} \dot{x} + (k - m\omega^2)x = mg \cos \gamma \sin \omega t \quad (2)$$

where  $m$  is the mass of the magnet,  $k$  is the effective spring constant of resonator (at different vibration modes),  $\beta$  is the damping coefficient,  $\omega$  is the angular speed, and  $\theta$  and  $\gamma$  are defined in the figure. The steady state motion of the magnet can be found to be:

$$x = mg \cos \gamma \sin(\omega t - \phi) / k \sqrt{(1 - 2\omega^2/\omega_n^2)^2 + \beta^2} \quad (3)$$

The above equation relates the displacement of the magnet mass to the rotation speed and angular position around a rotation disk. By analyzing the displacement of the magnet mass, we can obtain a first-order estimate of the power output from the transducer as done in [4]. It should be noted that, based on the above equation, the resonance occurs at  $(1/\sqrt{2})\omega_n$ , which is different from  $\omega_n$  for non-rotating vibration-based transducers.

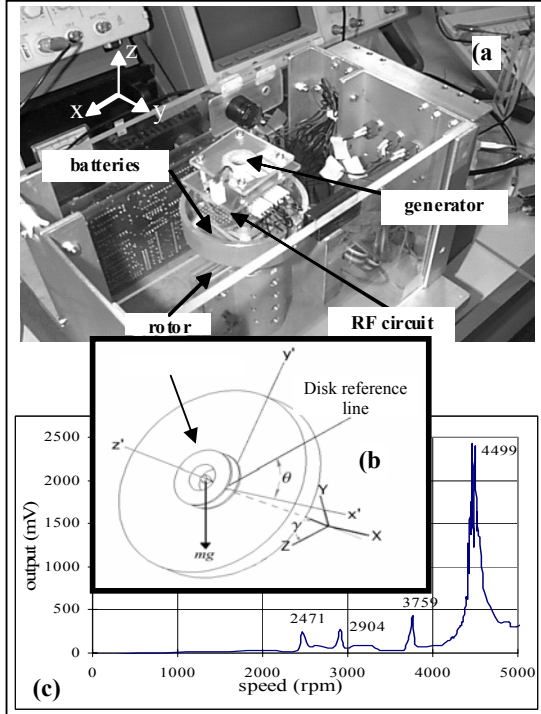


**Figure 9.** (a) The experimental setup to test the MPG output due to rotation. (b) Reference frames for the spring-mass dynamic analysis under rotation. (c) Experimental data showing the MPG voltage output at different rpms.

We used a wireless circuit and a custom-built rotation (Figure 9a) system to monitor the motion of the spring-mass under rotation [6]. An experiment was performed to find the effectiveness of the MPG as a power transducer using an 8cm diameter disc that underwent rotation about a horizontal axis. We should note here that if a mass is unbalanced above a rotational axis, vibrations can occur in the rotating object. These vibrations can be another source of excitation to the MPG. We have measured the vertical vibration of the custom-built rotation system using a Polytec OFV303 laser and an OFV3001 vibrometer controller. The data revealed that our test system has a natural frequency of 40Hz with an amplitude of  $117\mu\text{m}$ . We used this information to later deduce that the MPG's output voltage is dominated by its intrinsic rotational resonance rather than by the vibration of the test system.

An example of voltage output as a function of the rpm of the 8cm disc is provided in Figure 9c. The resonant frequency of the spring-mass is at 4500 rpm (75Hz). As predicted, the rotation resonance is lower

than its resonant frequencies due to vertical input vibration (i.e., for this spring-mass, 2<sup>nd</sup> mode is 88Hz, and 3<sup>rd</sup> mode is 97Hz). This is an indication that power output can be generated from the imbalance of gravitational and centrifugal forces of a mass undergoing rotation as well. An efficient generator should convert the mechanical vibration and force-imbalance energy sources into electrical energy. From our experiments, we have found that, for a  $1\text{cm}^3$  MPG, the total electrical power output from converting both the vibration and rotation-induced mechanical energy sources is sufficient to drive an RF wireless circuit system.

## SUMMARY

Thus far, we have shown at a  $1\text{cm}^3$  magnetic-induction based micro power transducer is capable of converting mechanical vibrations into electrical power sufficient to drive both IR and RF wireless circuit. Typical input mechanical amplitude needed is  $\sim 200\mu\text{m}$  at 100Hz to allow the transducer to generate enough power for wireless data transmission over 5m. We have also successfully developed a vibration-induced power generator which can be housed in an AA-size battery container. Efforts are underway to find specialized wireless applications for this AA-size power conversion cell. The main component of this power cell is a energy transducer made using MEMS compatible high-aspect-ratio SU-8 process. We have also shown that the generator can be implemented in a rotation system to generate sufficient power for RF transmission.

## ACKNOWLEDGEMENT

This work is funded by The Chinese University of Hong Kong and by a grant from the Hong Kong Innovation and Technology Commission (ITF/185/01). We also appreciate Magtech Industrial Company (Hong Kong) for donating and fabricating the magnets needed for this project. In addition, Cyberjet Technology (HK) Limited has provided invaluable assistance in developing the SU-8 molding technology used in this project.

## REFERENCES

- [1] P. B. Koeneman, I. J. Busch-Vishniac, and K. L. Wood, "Feasibility of Micro Power Supplies for MEMS", *IEEE/ASME J. MEMS*, Vol. 6, No. 4, December 1997.
- [2] C. B. Williams, and R. B. Yates, "Analysis of a micro-electric generator for microsystems", *Sensors and Actuators, A* 52, 1996, pp. 8-11.
- [3] R. Amirtharajah, and A.P. Chandrakasan, "Self-powered signal processing using vibration-based power generator", *IEEE J. of Solid-State Circuits*, vol. 33, May 1998, pp. 687-69.
- [4] W. J. Li, P. H. W. Leong, T. C. H. Hong, H. Y. Wong, and G. M. H. Chan, "Infrared Signal Transmission by a Laser-micromachined vibration-induced power generator", 43rd IEEE Midwest Symposium on Circuits and Systems, August 8-11, 2000, Michigan, USA.
- [5] N. N. H. Ching, H. Y. Wong, W. J. Li, P. H. W. Leong, and Z. Y. Wen, "A laser-micromachined multi-modal resonating power transducer for wireless sensing systems", *Sensors and Actuators, A: Physical*, 2002, pp. 685-690.
- [6] T. K. H. To, W. Sun, and W. J. Li, "A wireless self-powered rotation sensing system using a vibration-based micro power transducer", *IEEE/ASME M2VIP*, Hong Kong, Aug 27-28, 2001.